J|A|C|S

A R T I C L E S

Organocations in Zeolite Synthesis: Fused Bicyclo [*l.m*.0] Cations and the Discovery of Zeolite SSZ-48

Greg S. Lee,§ Yumi Nakagawa,† Son-Jong Hwang,⊥ Mark E. Davis,⊥ Paul Wagner,⊥
Larry Beck,# and Stacey I. Zones*

*Contribution from the Chevron Research and Technology Center, 100 Chevron Way,
P.O. Box 1627, Richmond, California 94802, and Department of Chemical Engineering,
California Institute of Technology, Pasadena, California 91125*

Received June 21, 2001

Abstract: A set of zeolite synthesis experiments is described where lattice substitution is varied in the context of the structure of particular structure-directing organocations (at times referred to as templates). In this particular series, the organocations are constructed as members of a fused bicyclo organonitrogen class of compounds, described as having ring construction [*l.m.n*], where $n = 0$. We show that these compounds can best be achieved from starting cyclic ketones that are converted to imines via a Beckman rearrangement reaction. A particular approach to the Beckmann reaction works best in our hands. In some instances isomeric organocations are made and separated. Often their use in zeolite synthesis led to different products. There is a high correlation for the space-filling details of the guest organocations and the type of crystalline host lattice developed in the synthesis. In one instance involving isomers of a decahydroquinoline derivative, a new zeolite, SSZ-48, is discovered and contains only one of the isomers. Characterization of the isomers and their use in the zeolites is followed by ^{13}C MAS NMR analyses. Some details of the new zeolite are given and it is shown that a reasonable symmetry operation predicting a 14-ring zeolite could be generated under similar conditions to SSZ-48 (a 12-ring zeolite).

Introduction

Our research programs in zeolite synthesis, carried out at Caltech and the Chevron Research and Technology Center, have been engaged for a while in trying to understand the key mechanisms. We have explored how both the inorganic chemistry[1] and classes of organocations[2−5] can affect the eventual crystalline product. In particular we have been intrigued with the possibility that zeolite formation with a guest molecule and a surrounding host lattice may develop from molecular self-assembly chemistry. While the guest molecule can have a very pronounced effect on the eventual host inorganic lattice formed, there is surprisingly little difference in the energetics for the formation of these high silica materials. Earlier studies on enthalpies of formation[6] have been followed by recent calorimetric measurements designed to yield entropy comparisons.[7] The emerging data seem to point toward a "kinetic-control"

process in these crystallizations. The ability to stabilize viable nuclei, from perhaps a spectrum of guest−host configurations, may determine which crystalline product forms.[8,9]

Figure 1 shows a schematic model of how organocations, heated in a closed reaction containing SiO_2, alkali hydroxide, and water, may begin to organize an inorganic lattice. We will see in this study that minor substitution for Si with B or Al also can alter the nuclei stabilized, leading to changes in crystalline phase selectivity. Control of the pore properties features and the size and morphologies of zeolite crystals are, of course, important for their use in industrial applications, where zeolites stand out as shape-selective solid acids usable at high temperatures.[10−12]

Recently we have been describing organic guest and inorganic host−lattice chemistry leading to crystallization of new high-silica zeolite structures with either aluminum or boron trivalent substitution in the tetrahedral positions comprising the lattice. In two recent studies we described systematic approaches to extend the size of single ring, charged heterocycles to move the resulting zeolite products away from clathrasil or one-dimensional, parallel pore molecular sieves. These are generally the favored high-silica, guest/host crystallization products.[13] In

* Corresponding author. Chevron Research and Technology Center. E-mail: sizo@chevrontexaco.com.
§ Current address: Lawrence Livermore National Lab, Livermore, CA.
† Current address: Chiron Technologies, Emeryville, CA.
⊥ California Institute of Technology.
Department of Chemistry, University of Michigan.

(1) Davis, M. E.; Zones, S. I. In *Synthesis of Porous Materials*; Occelli, M. L., Kessler, H., Eds.; Marcel Dekker: New York 1997; p 1.
(2) Wagner, P.; Nakagawa, Y.; Lee, G. S.; Davis, M. E.; Elomari, S.; Medrud, R. C.; Zones, S. I. *J. Am. Chem. Soc.* **2000**, *122*, 263−273.
(3) Zones S. I.; Nakagawa, Y.; Yuen, L. T.; Harris, T. V. *J. Am. Chem. Soc.* **1996**, *118*, 7558−7567.
(4) Nakagawa, Y.; Zones, S. I. In *Molecular Sieves*; Occelli, M. L., Robson, H. E., Eds.; Van Nostrand Reinhold: New York, 1992; Vol. 1, p 222.
(5) Zones, S. I. *Zeolites* **1989**, *9*, 458−467.
(6) Petrovic I.; Navrotsky A.; Zones S. I.; Davis M. E. *Chem. Mater.* **1995**, 5.
(7) Piccione, P. F.; Woodfield, B. F.; Boerio-Goates, J.; Navrotsky, A.; Davis, M. E. *J. Phys. Chem. B.* In press.

(8) Barrer, R. M. *Hydrothermal Chemistry of Zeolites*; Academic Press: London, 1992; Chapter 4.
(9) Harris, T. V.; Zones, S. I. *Proceedings of the 10th International Zeolite Conference;* Garmisch, Elsevier: Amsterdam, The Netherlands, 1994; p 29.
(10) Jansen, J. J.; Coker, E. In *Molecular Sieves*; *Science and Technology*; Karge, H. G., Weitkamp, J., Eds.; Springer-Verlag: Berlin, Germany, 1998; Vol. 1 "Synthesis", pp 121−156.
(11) Miller, S. J. *Wax Isomerization for Improved LubeOil Quality*; AICHE Spring Meeting, New Orleans, LA, March 1998.
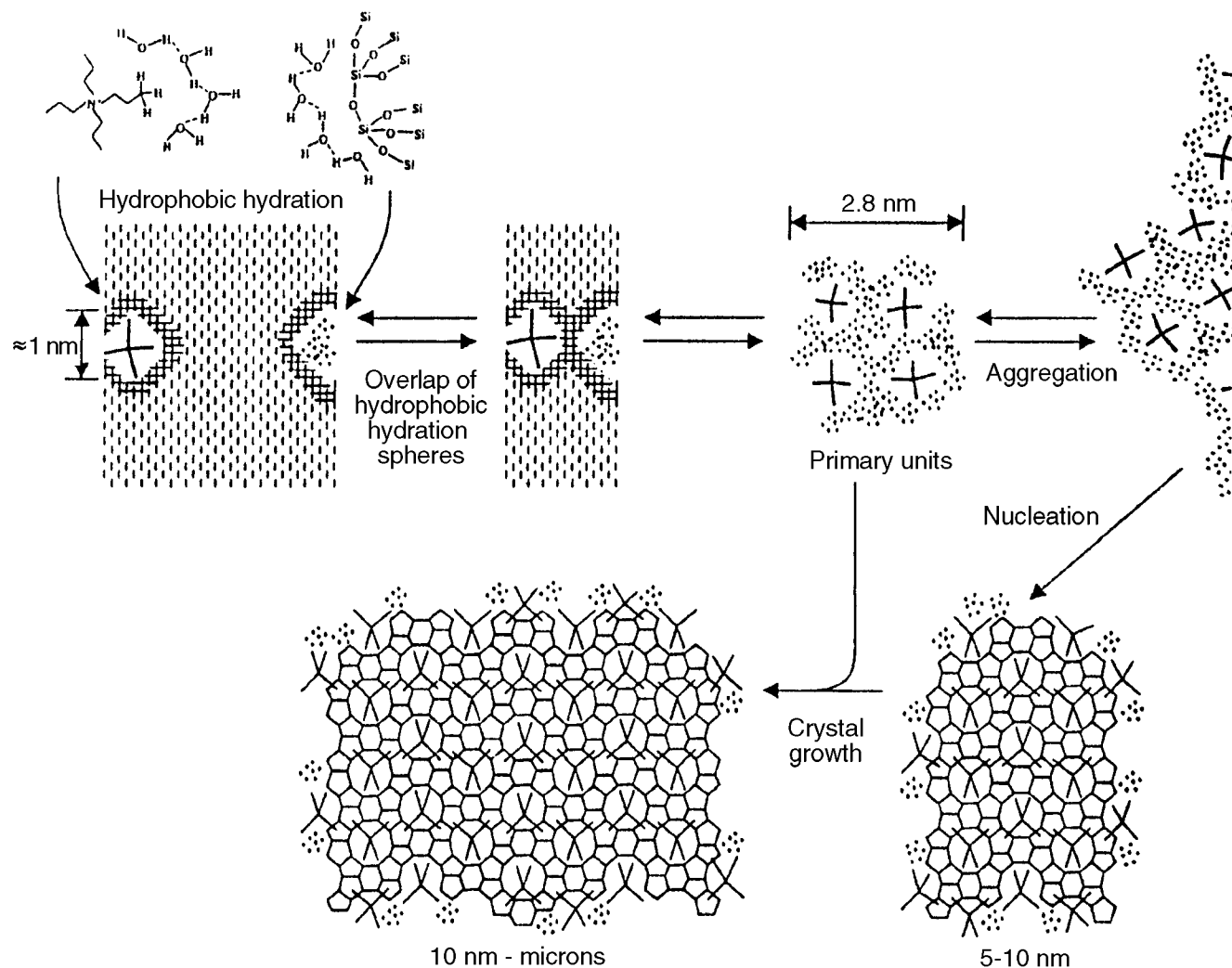(12) Barger, P. T.; Wilson, S. T.; Holmgren, J. S. U.S. Patent 5,126,308, 1992.

Figure 1. Proposed mechanism for the nucleation of Si-TPA-MFI.

the first study, piperidine derivatives were examined with variation of ring substitution on both carbon and nitrogen. In the latter instance some examples of spiropiperidines were given; one led to a very surprising discovery of a spiro compound mimicking trimethyl-1-adamantammonium cations in the selectivity to zeolite SSZ-23.[14]

A second study examined bicyclo (as well as tri- and tetracyclo) organocations where bridging carbons were a key feature. The guest molecules were bicyclo [*l.m.n*] compounds where no value equaled 0. Figure 2 depicts this type of polycyclic ring construct and it can be seen that two atoms are shared by each of the larger completed rings. These two atoms are the bridging atoms. The examples given then show the atoms connecting the bridging atoms as 0, 1, 2, and 3 different zeolite products are obtained. This group of molecules favored the formation of "cage-based" zeolites. The relationship of lattice substitution and nucleation of zeolites SSZ-36 (large cage, 8-ring portals) and SSZ-35 (large cage, 10-ring portals) was discussed.[2] The latter zeolite was favored for most guest molecules used at the higher SiO_2/Al_2O_3 ratio synthesis conditions.
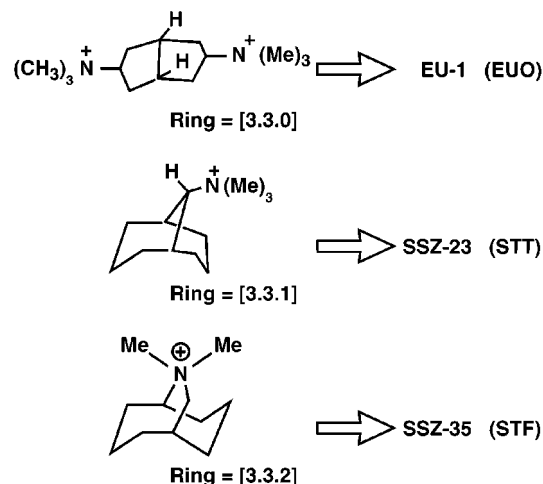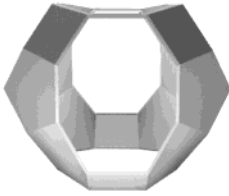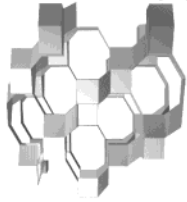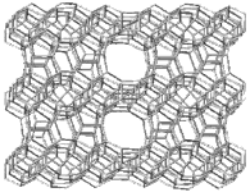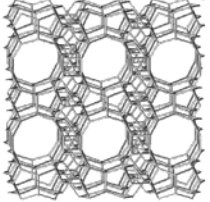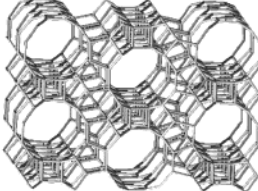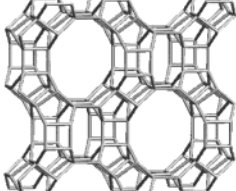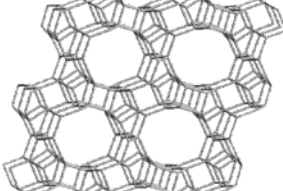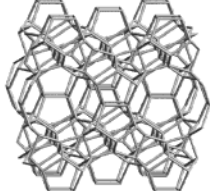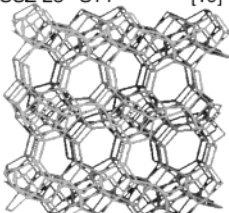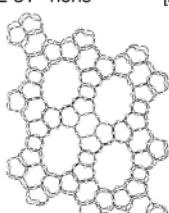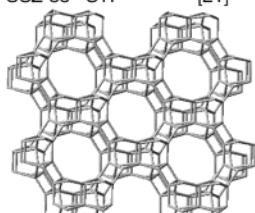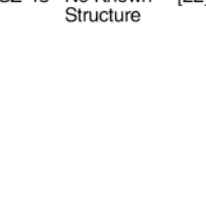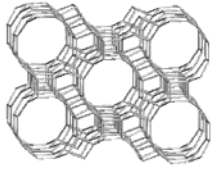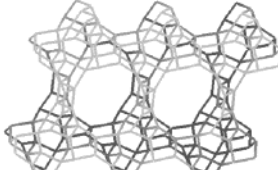

Figure 2. Examples of quaternary ammonium cations based upon bicyclo [*l.m.n*] ring systems. Examples of [3.3.0], [3.3.1], and [3.3.2] are given as well as the zeolites made from the candidate "template" or structure-directing agent (SDA).

Table 1 shows structural representations of all the zeolites discussed in this study. We also include an International Zeolite Association Structure Code when one has been assigned. We also give ring-size and comments. 8-rings and 6-rings usually

(13) Nakagawa, Y.; Lee, G. S.; Harris, T. V.; Yuen, L. T.; Zones, S. I. *Microporous Mesoporous Mater.* **1998**, *22*, 69−85.
(14) Camblor, M. A.; Diaz Cabanas, M.-J.; Perez-Pariente, J.; Teat, S. J.; Clegg, W.; Shannon, I. J.; Lightfoot, P. A.; Morris, R. E. *Angew. Chem., Int. Ed.* **1998**, *37*, 2122.

Table 1. Zeolites Made and References

Zeolite	IZC Code	Reference
SSZ-36	ITE/RTH	[2]

8X8-ring, 3D representation

Zeolite	IZC Code	Reference
SSZ-13	CHA	[19]

8-ring, 3D representation

Zeolite	IZC Code	Reference
EU-1	EUO	[19]

10-ring, side pockets

Zeolite	IZC Code	Ref.
SSZ-37	NES	[19]

10-ring, side pockets

Zeolite	IZC Code	Reference
BETA	BEA	[19]

12x12x10-ring

Zeolite	IZC Code	Reference
Mordenite	MOR	[19]

12x8-ring

Zeolite	IZC Code	Reference
ZSM-12	MTW	[19]

12-ring

Zeolite	IZC Code	Reference
Nonasil	NON	[19]

6-ring

Zeolite	IZC Code	Reference
SSZ-23	STT	[19]

9x7-ring

Zeolite	IZC Code	Reference
SSZ-31	none	[20]

12-ring

Zeolite	IZC Code	Reference
SSZ-35	STF	[21]

10-ring

Zeolite	IZC Code	Reference
SSZ-43	No Known Structure	[22]

12-ring?

Zeolite	IZC Code	Reference
SSZ-26	CON	[23]

12x10-ring

Zeolite	IZC Code	Reference
SSZ-48	SFE	[24]

12-ring

have apertures near 4.5 and 2.6 Å, respectively. 10-rings are in the 5−6 Å range. 12-rings can be 6−7.5 Å. A reference is also given where more information can be obtained about the given zeolite.

We next considered what happens if two rings are fused together in developing the organocation guest and the charge resides within one ring. In this instance there are once again two carbon (one may be nitrogen) atoms, which are bridging because they belong to both rings. But unlike the above-mentioned system, there are no atoms between the bridge points, just a single bond. These materials constitute the case for bicyclo [*l.m.*0] systems and Figure 3 depicts this type of molecule. Both a cis and a trans configuration are possible in terms of the two fused rings. The trans isomer has more of the atoms comprising the rings sitting parallel to a single plane; its geometry can be said to be more planar.

We have previously discussed the advantage of using rigid, polycyclic guest molecules, to fix their conformation with more certainty. Molecules that are floppy or have considerable
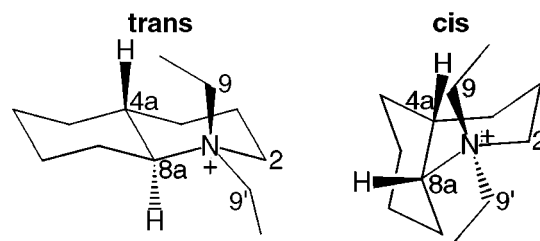
Figure 3. Differences in cis (right) and trans (left) configurations for bicyclo cations **15** and **16** as examples of the [4.4.0] system.

flexibility around certain axes have a better chance to serve as guests for the crystallization of parallel, one-dimensional pore zeolites such as ZSM-12 (MTW code). In these channel-based zeolites the pore aperture is the same dimension as occurs on down the channel. The channels are parallel but nonintersecting. The situation is often visualized as a group of straws placed parallel and in a bundle. A series of molecules built by using piperidine cores but with flexible methylene chains involved

Figure 4. (a) Zeolite ZSM-12 (MTW), 1D channel structure. Parallel channels are shown at the right. (b) SSZ-35 (STF) and SSZ-44 (SSF) as examples of cage-based zeolite structures.

nicely demonstrated this feature.[15] Figure 4a shows the topological features for ZSM-12. In contrast we also show SSZ-35 (STF), a "cage-based" zeolite structure, in Figure 4b. The cage-based materials have a cage or cavity repeated periodically within the structure. These have larger cross-section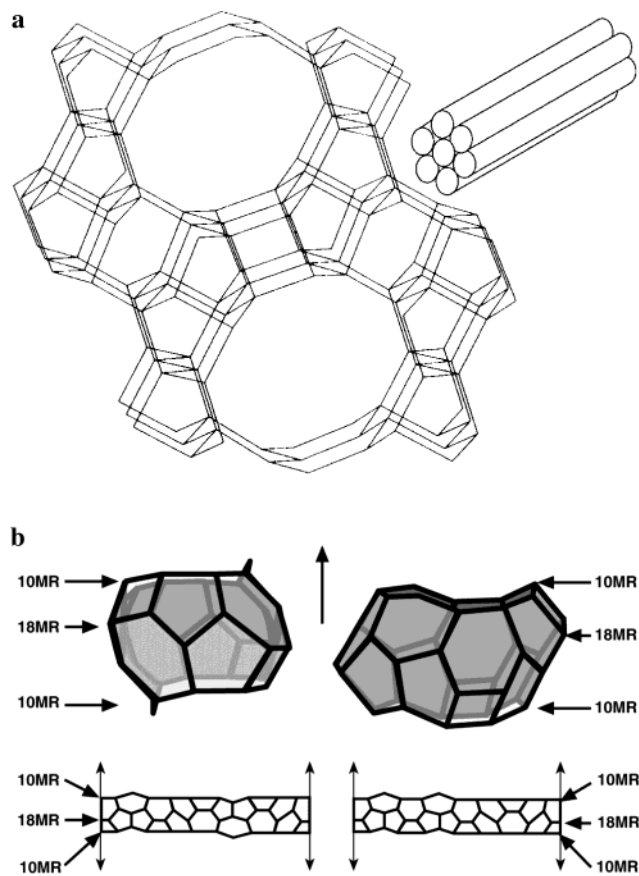s than the pore openings into the zeolite. By definition this would certainly occur whenever channels intersect within the zeolite. This occurs in β zeolite, for example. There are also examples of zeolites (STF is one) where the larger cages have formed but do not connect from one channel into another; they remain isolated but larger than the pore mouth. Here it is tempting to imagine that the organocation begins the nucleation of the host structure by organizing a silicate cage around itself.

In this report we examine the fused bicyclo system with the capability of generating some larger rings and making more than one positional isomer for charged nitrogen, within a ring. This latter opportunity derives from the combined use of the Beckmann rearrangement carried out on cyclic ketones and the ability to separate the imide isomers formed. This was true in most but not all syntheses carried out. In a few cases the mixture was propagated onto the organocation stage and tested as such. In the work reported a new zeolite SSZ-48 is described. While the discovery initially occurred in a system using just these types of mixed isomeric guest molecules, it will be shown that only one of the two isomers is responsible for crystallizing SSZ-48. Isolation of the minor isomer and testing it alone led to a different set of zeolite crystallization products.
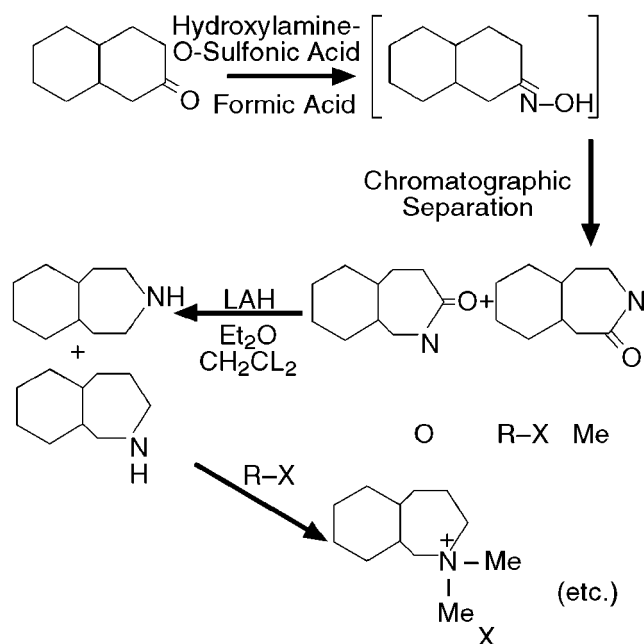
(15) Tsuji, K.; Davis, M. E. *Microporous Mesoporous Mater.* **1997**, *11*, 53.

Figure 5. A general organic synthesis scheme for the preparation of bicyclo [*l.m.n*] systems, using a Beckmann rearrangement strategy.

Table 2. Bicyclo [*l.m.*0] Organocations Used in Zeolite Synthesis

Entry	Structure	[m, n, O]	Reactant SiO₂/M*₂O₃ = 25	50	75	100	200
1		[5.4.0]	SSZ-13	SSZ-13	SSZ-37	♦	SSZ-31
2		[5.4.0]	Beta	Beta	MTW	MTW	MTW/31
3		[6.4.0]	SSZ-36	SSZ-31	SSZ-31	SSZ-31	SSZ-31
4		[5.4.0]	SSZ-36	♦	SSZ-36	SSZ-36	♦
5		[6.3.0]	Beta	Beta/Euo	Euo/Beta	⟶	Euo
6		[6.3.0]	MORD/MTW	MTW	MTW	MTW	MTW
7		[6.3.0]	Beta	Beta/MTW	MTW/Beta	MTW	MTW
8		[4.4.0]	SSZ-13	SSZ-13,36,35	SSZ-13,43	SSZ-35	♦
9		[4.4.0]	Beta	SSZ-43	SSZ-43	♦	SSZ-43
10		[4.4.0]	SSZ-26?	SSZ-48	SSZ-31	♦	SSZ-31
11		[4.3.0]	SSZ-13/ ANA	NON	NON	♦	MTW/SSZ-31
12		[4.3.0]	SSZ-13	NON	NON	NON	NON/MTW
13/14		[5.4.0]	Beta	MTW	MTW	MTW	MTW MTW

♦ = no product formed
*(where M = Al or B)

Experimental Section

1. Synthesis of Organocations. Eleven different organocations were prepared from starting bicyclo ketones, using the Beckmann rearrangement route outlined in Figure 5. This reaction chemistry was optimized for bicyclic ketones, using the method of Fung and Olah.[16] NMR and elemental analyses characterized the products. A synthesis and isomer separation for entries **1** and **2** of Table 2 is as follows:

2-Decalone was (Aldrich Chemical Co., 101 g) mixed in a three-neck, 2 L reaction flask with 633 g of 96% formic acid. Stirring was carried out with a magnetic stir bar. From a sidearm addition funnel,

(16) Olah, G.; Fung, A. P. *Synthesis* **1979**, 537.

110 g of hydroxylamine-*o*-sulfonic acid (Aldrich) in 317 g of formic acid was added dropwise. The addition was carried out over about 15 min and a slight exotherm developed. The reaction is heated to reflux.

Overnight the reaction went from a pale yellow solution to black. TLC (98/2 CHCl₃/CH₃OH on silica) showed the reaction was complete. The reaction was carefully poured onto 2 kg of ice and then carefully, the pH was raised to about 12 with 50% NaOH solution. This aqueous phase was next extracted 3 times with methylene chloride and these extracts were dried with sodium sulfate. The dried extract was then stripped under reduced vacuum, leaving 78 g of dark oil that crystallized. The dark oil, a potential mixture of two imide isomers, was further purified by column chromatography. The crude material was dissolved in a minimum of methylene chloride and then loaded onto a silica gel (230−400 mesh), 1 kg, loaded in a slurry with chloroform. About 6 L of 98/2 chloroform/methanol was run over the column and multiple fractions were collected and analyzed by TLC. 61 g of light brown solid were recovered.

The mixture of imides was reduced with lithium aluminum hydride (LAH). A 5 L three-neck round-bottom flask equipped with an overhead mechanical stirring system was used. The 61 g of product from the column purification was dissolved in methylene chloride and this solution was added dropwise to the main flask, which already contained 1.1 L of anhydrous ether and 44 g of LAH (Aldrich). As the addition began, there was an exothermic evolution of gas. The reaction temperature was controlled by the use of an acetone/dry ice bath around the flask. The addition was carried out over 0.5 h. The dry ice bath was removed so that the reaction could come to room temperature slowly. The reaction was then stirred overnight at room temperature.

The next day, 44 g of water was slowly added dropwise with much gas evolution. Some additional methylene chloride was added to make up for the volume of ether lost (in the hood!) from the gas evolution. 44 g of 15% NaOH solution was added next. This was followed by the addition of 131 g of water while good stirring was maintained throughout. The white solid byproduct was washed with methylene chloride and this wash was added to the existing two-phase system after solids were removed by filtration. The methylene chloride extract was dried with sodium sulfate. Recovery of the product from removal of solvent gave an oily solid. This was treated with ether and the remaining solids were filtered. Separate workup of the ether extract gave 42 g of an orange oil.

A 21 g sample of the oil was converted into the mixture of **1** and **2** by reaction with 58 g of methyl iodide (added dropwise) to 20.4 g of potassium bicarbonate and the oil in 140 mL of methanol. This alkylation was carried out at room temperature for over a week. The reaction was stripped down to dryness and the product was recovered into chloroform. The product was then obtained by removal of the chloroform.

The two isomers were separated by fractional recrystallization from hot acetone and methanol combined. The first crop consisted of **1**. A subsequent crop yielded isomer **2**. ¹³C NMR of the products verified the separate identity.

In some instances, when isomers arose from the Beckmann rearrangement, a separation was carried out at the imide stage, using column chromatography. A typical procedure was to dissolve the mixture in a minimum of chloroform, load it onto a column of silica gel (230−400 mesh), and elute with 2%, 98% methanol/chloroform.

In other cases, the product can be prepared from available cyclic amines such as decahydroquinoline. A representative procedure is as follows: The two different isomeric decahydroquinoline derivatives (cations **15** and **16**) were prepared by ethylation of the decahydroquinoline. Decahydroquinoline (24.8 g; Aldrich, mixture of isomers) was dissolved in 170 mL of methanol. Potassium bicarbonate (26 g) was slurried into this solution in a 500 mL round-bottom flask, stirred by use of a magnetic stir bar and hot plate. Using a dropping funnel with an equalizer arm, 67.4 g of iodoethane was added dropwise over a 15-min period. No exothermal reaction was detected for this room

temperature addition. With a heating mantle, the reaction was slowly brought to reflux in the presence of a condenser. Heating was continued for 2 days. After cooling the mixture to room temperature and stripping off the methanol, the solids were triturated with 250 mL of chloroform (to extract the product away from inorganic solids). Organocations were recovered from removing the chloroform and were then recrystallized in a minimum of hot isopropyl alcohol. The collected product was a mixture of isomers (cis and trans configurations). A further crystallization from hot methanol/acetone (see above) yielded a separation with the first and second crop consisting of the two separate isomers, **15** and **16**.

The iodide salt was converted into the hydroxide form via treatment with BioRad AG 1-X8 hydroxide exchange resin. The zeolite syntheses were carried out with use of the hydroxide form. Cations **8−10** were similarly prepared with different alkylation reagents.

2. Zeolite Synthesis. The conditions for synthesizing zeolites in the presence of these organocations recently have been described by us in a prior publication.[2] A representative example was given for each of the 5 SiO₂/Al₂O₃ ratios. One example of synthesis with sodium borate was also described.

In a representative zeolite synthesis, for the SiO₂/Al₂O₃ = 100 example, the reagents are combined in the Teflon cup of a Parr Chemical Company 23 mL Stainless steel reactor. Reheis F-2000 alumina hydroxide (0.03 g, 53% Al₂O₃) was dissolved in a basic solution composed of 2.15 mmol of the organocation as the hydroxide form and 1.5 mmol of sodium hydroxide, both bases in a total of 11.75 g of water. Cabosil M-5 (0.90 g, 97% SiO₂) was blended into the solution. The reactor was sealed and heated at 170 °C and rotated at 43 rpm for 6−12 days. When solids settled on the bottom of the cup, the contents were washed in a filter, dried, and examined by powder X-ray for phase determination.

3. Characterization of Zeolite Crystallization Products. The zeolite products were characterized initially by X-ray powder diffraction. Experiments were run on a Siemens D-500 instrument. Further characterization was carried out, in particular the relationship to SSZ-48. The data taken at the Brookhaven National Lab Beamline were from a sample that had been calcined to 600 °C, then loaded into a 1 mm capillary tube which was sealed while under vacuum and at 350 °C. The X7A synchrotron beamline was used for data collection.

4. Microscopy. The scanning electron micrographs were taken on a Hitachi S-3200 instrument. The TEM micrograph was taken on a JEM 4000-EX, using techniques that have been described.[17]

5. NMR. One- and two-dimensional ¹H and ¹³C NMR spectra were obtained for the organocations in solution (CDCl₃) on a Varian INOVA-500 (500 MHz for ¹H, 125 MHz for ¹³C) spectrometer. ¹³C cross polarization magic angle spinning (CPMAS) spectra of the iodide salts (prior to hydroxide ion-exchange) were recorded on a Bruker DSX-500 MHz spectrometer, using a 4 mm CPMAS probe (detailed experimental parameters are given in figure captions). The ¹³C MAS and CPMAS experiments were performed for as-synthesized zeolites using a Bruker DSX-200 (200 MHz, 50 MHz) or a Bruker AM 300 spectrometer that was modified for solid NMR measurements.

Results and Discussion

1. Generation and use of [*l.m*.0] Organocations. Figure 5 gives a scheme for the organic synthesis of candidate molecules starting from 2-decalone (a [4.4.0] ring system). One can see that the eventual Beckmann rearrangement lactam provides for a ring expansion into a [4.5.0] system. The scheme depicts starting with a ketone at the 2 position and generating isomeric amides at the 2 and 3 positions. A discussion of the reaction product probabilities for different systems has been given by Krow.[18] In our work, we found this combination to give superior

(17) Wagner, P.; Terasaki, O.; Ritsch, S.; Nery, J. G.; Zones, S. I.; Davis, M. E.; Hiraga K. *J. Phys. Chem. B* **1999**, *103*, 8245−50.

results, allowing our yields to be high enough to move on to subsequent steps.

Retention of configuration is maintained during the reduction to the amine. In the meanwhile we have not yet discussed the issue of whether we could be dealing with a cis/trans conformer with regard to ring stereochemistry (see Figure 2). However, the transformation steps used in the Beckmann rearrangement do not affect the stereochemistry around the 2-ring fusion carbons. If we start with a cisoid ketone that configuration will be retained for a number of reagent choices for carrying out the Beckmann rearrangement reaction.

Using this synthesis route, a number of organocation guest molecules were generated and then tested in zeolite synthesis reactions. As in some past studies from our lab[2] we attempted to scope out zeolite crystallization selectivity as a function of lattice substitution (in most cases Al). A set of results is given in Table 2. We show the structure of the organocation guest, the particular [*l.m.*0] system to which it belongs, and then the zeolites found in the crystallization reactions. In total, as many as 13 different high-silica structures can be developed from these 14 organocations, often depending upon the lattice substitution as well as the geometry and charge positions of these cations. Some crystallization product maps, where we juxtapose the synthetic relationship of the inverse function of OH/SiO$_2$ vs SiO$_2$/M$_2$O$_3$ where M = B or Al (product or reactant),[1] help to highlight certain organocation structure-directing features. Figure 6 shows these product transitions with regard to these ratios for the pairs, 2 and 3 N + [4.5.0] bicyclo cations (entries **1** and **2** in Table 2). The more symmetric 3-derivative shows a transition for producing β zeolite at high OH/SiO$_2$ and higher lattice substitution, giving way to the parallel pore 1D system of MTW at higher SiO$_2$/M$_2$O$_3$, where M = B or Al, ratios. We have seen this trend before for some other organocations.[3] The less symmetric 2-derivative leads to an entirely different set of products. At the high substitution end, the highly microporous SSZ-13 (Chabazite structure) is found. With changes in synthesis conditions, the products transition to SSZ-37 (NES structure) and then to SSZ-31.[20] At the highest SiO$_2$ values this latter zeolite is also 1 D, but interestingly has a larger (than MTW), elliptical pore to incorporate the bulkier 2-derivative. So a good correlation for spatial parameters for the organocation and the subsequent features for the crystallizing zeolite is observed in the use of this isomeric pair.

Figure 7 now compares the same ring structures but with *N*-diethyl substituents (entries **4** and **14**) instead of the dimethyls seen in Figure 6. For the more symmetric 3 − *N* derivatives, the same product transition is seen again. That is BEA to MTW. This indicates that additional filling down a channel is not altering the structure in either instance. With the bulkier and less symmetric 1 − *N* derivative, the products are altered. None of the previous 3 zeolites (SSZ-13, -37, -31) are seen, but the consistent product is now SSZ-36. We previously showed that this material has a very large cavity and high microporosity, and is interwoven with a network of 8-ring (small pore) channels.

Figure 8 compares three organocations each built from the [6.3.0] system with N at the 2 position. These are now
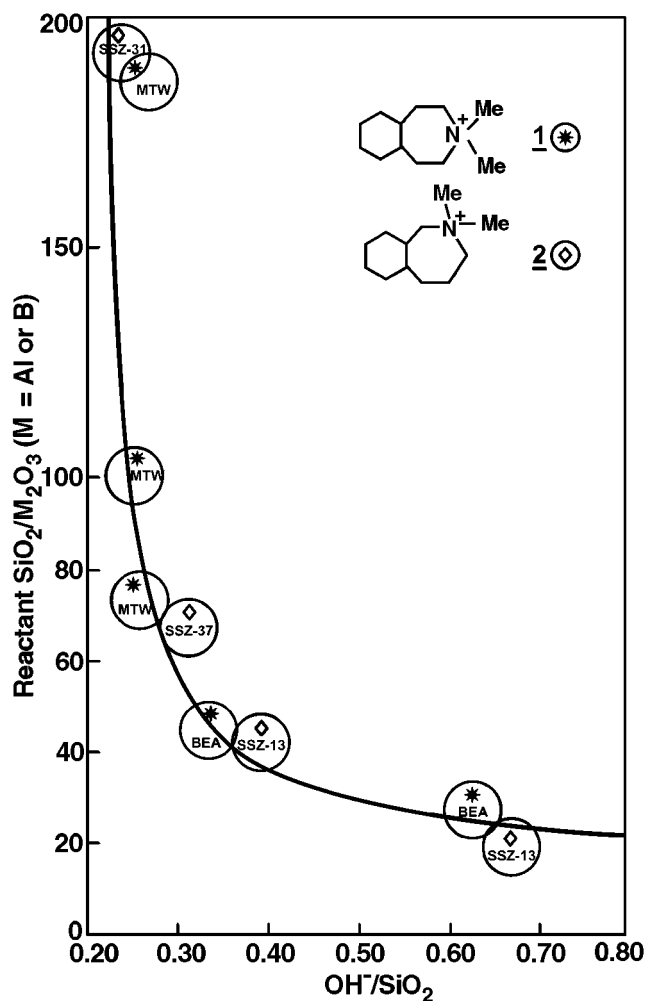

Figure 6. A comparison of the types of zeolites made using isomeric compounds **1** and **2**. The zeolite products change with respect to the inverse functions OH$^-$/SiO$_2$ in reactants and SiO$_2$/Al$_2$O$_3$ in products as shown in our curve.

symmetric relative to a long single axis. The three derivatives are not necessarily symmetric with regard to substituents. The smallest, *N*-dimethyl derivative (**7**) yields the familiar β to MTW transition, over the course of the five lattice substitution ratio syntheses. Adding an ethyl group, at the expense of one of the methyls (**6**), removes β at high substitution, but MTW is still the product in reactions. However, if the ethyl is replaced in turn with an isobutyl group (**5**), the 1D MTW is lost entirely. At the highest substitution, β is the product and then the higher silica default is the EUO zeolite. It is surprising to see this product at the SiO$_2$/Al$_2$O$_3$ (SAR) ratio of 200. One also suspects that with further experimentation the ethyl derivative could be found to select β zeolite under some high lattice substitution conditions.

Table 3 brings together the results from one entry from Table 2, with the two isomeric decahydroquinoline derivatives. The latter two can be thought of as [4.4.0] systems, and the additional material as [4.5.0]. The product selectivities are fascinating. The [4.5.0] organocation (**4**) has a very high selectivity for SSZ-36. The trans isomer of [4.4.0] (**16**; we will later show the similar trans relationship for [4.5.0]) yields either SSZ-13 or -36. The

(18) Krow, G. *Tetrahedron* **1981**, 1283−1307.
(19) Meier, W. M.; Olson, D. H.; Baerlocher Ch. *Atlas Of Zeolite Structure Types*, 4th ed.; Elsevier: London, 1996.

(20) Lobo, R. F.; Tsapatsis, M.; Freyhardt, C. C.; Chan, I. Y.; Chen, C. Y.; Zones, S. I.; Davis, M. E. *J. Am. Chem. Soc.* **1997**, *119*, 3732.
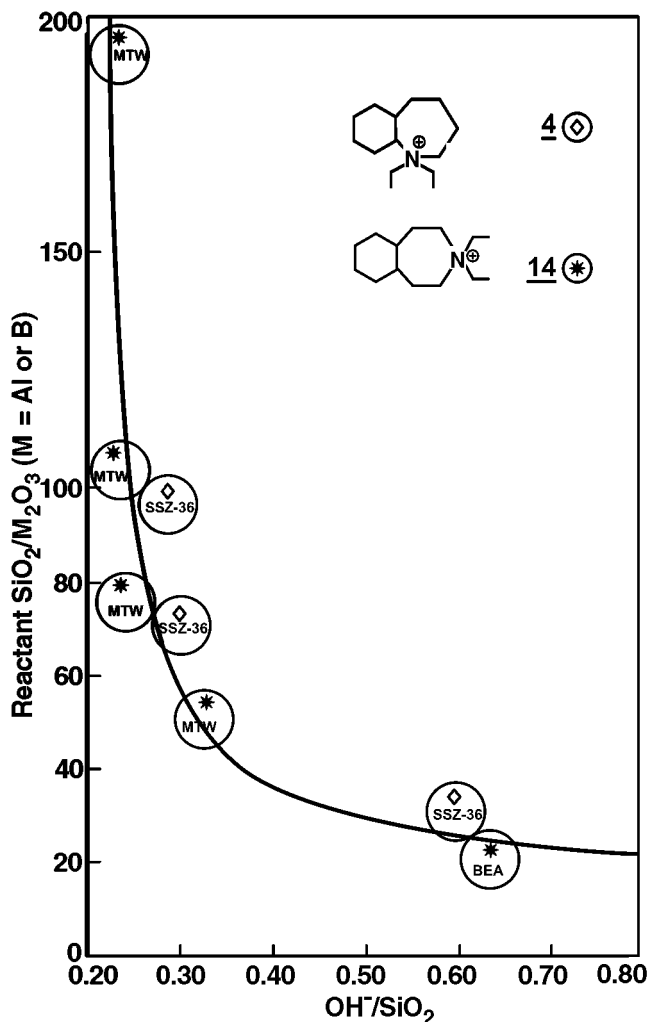
Figure 7. The same bicyclo ring structure used in compounds **1** and **2** is tested as the diethyl substituent. **4** has a high selectivity for SSZ-36, spanning both the high and low Al substitution regions.

Figure 8. A comparison of products formed (as in Figures 6 and 7) for SDA based upon different N-substituents for a bicyclo [6.3.0] system (entries 5−7). Zeolites β and mordenite are favored by high lattice substitutions, giving way to ZSM-12 (MTW) and EU-1 (EUO) with a decrease in OH^-/SiO_2 and reactant Al.

cis isomer (**15**), however, yields four different zeolites, three of which possess large pores and the fourth (SSZ-35) has 10-rings connected to each other through shallow 18-ring cavities. The SSZ-48 is forming in a borosilicate reaction with the reactant ratio of $SiO_2/B_2O_3 = 50$.[24] Also, this is only the second template organocation found to make aluminosilicate SSZ-26.[25] It should be also noted that the related organocation, **10**, can also make three of the four zeolites seen in syntheses with **15**. In a way it is a more rigid, tethered version of **15** so it is not surprising that the zeolite products would be similar.

One further point can be made about this class of organocations. With these bicyclo [*l.m.*0] compounds and each ring being 5 or larger, no 10-ring zeolites were obtained of the conventional variety. For example, simple heterocycles such as pyrrolidine, piperidine, morpholine, or pyridine can all be used in the synthesis of 10-ring zeolites with apertures in the 5 to 5.5 Å range and channels of the same size. These classes of
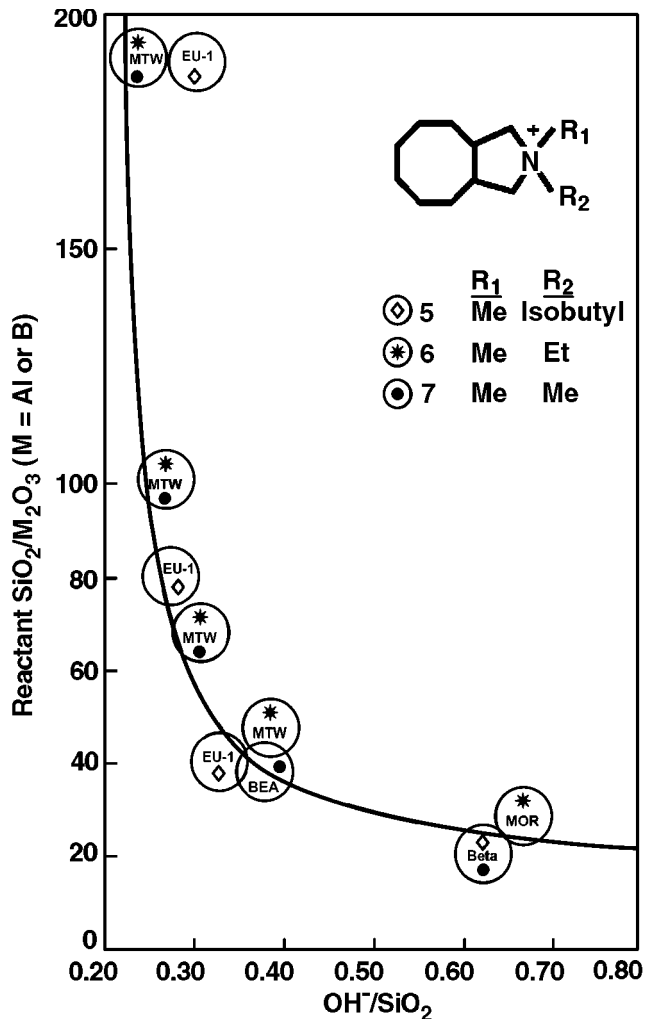
Table 3. Decahydroquinolines (from Figure 3)

	$SiO_2/M_2O_3{}^a =$				
compd	25	50	75	100	200
15	SSZ-26	BSSZ-48	SSZ-35	SSZ-31	SSZ-31
16	SSZ-13	-	SSZ-36		
4	SSZ-36	-	SSZ-36	SSZ-36	

^{a} Where M = A1 or B.

organocations we describe are too large to fit into such hosts. In preliminary studies where one of the fused bicyclo rings is a pyrrolidine component, we fail to obtain 10-ring zeolites. Rather the guest molecule packs into a clathrate structure like Nonasil or down the channel of MTW, depending upon the ring position of nitrogen substitution.

In the instance where a 10-ring was encountered in this work, SSZ-35 from **8** and **15**, the structure is actually more a sequence of shallow 18-ring cavities connected by 10-ring portals.

2. NMR Studies. The differences in product selectivities in Table 3 prompted us to be sure which of the two isomers (**15** or **16**) was responsible for crystallizing SSZ-48. We had seen that only one of the two produced SSZ-48 and the other led to zeolite SSZ-36 under the same synthesis conditions. The solution

(21) Wagner, P.; Zones, S. I.; Medrud, R. C.; Davis, M. E. *Angew. Chem., Int. Ed.* **1999**, *38*, 1269.
(22) Nakagawa, Y.; Lee, G. S. U.S. Patent 5,965,104, 1999.
(23) Lobo, R. F.; Pan, M.; Chan, I. Y.; Li, H.-X; Medrud, R. C.; Crozier, P. A.; Davis, M. E.; Zones, S. I. *Science* **1993**, *262*, 1543.
(24) Lee, G. S.; Zones, S. I. U.S. Patent 6,080,382, 2000.
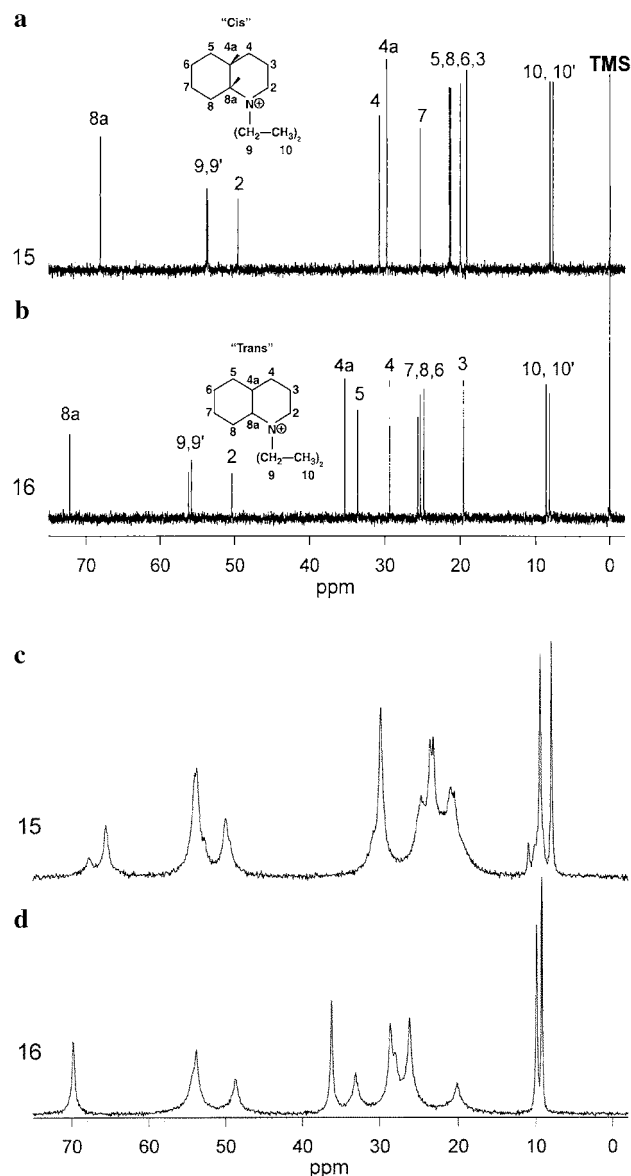(25) Zones, S. I.; Santilli, D. S.; Olmstead, M. M. *J. Am. Chem. Soc.* **1992**, *114*, 4195.

Figure 9. ^{13}C NMR spectra for the cis and trans isomers **15** and **16**: (a) **15** in solution (CDCl$_3$) and (b) **16** in solution (CDCl$_3$). Solid-state spectra were taken on iodide salts. (c, d) ^{13}C CP MAS spectra of **15** and **16** measured on a Bruker DSX-500. Contact time = 0.5 ms; spinning rate = 8.0 kHz.

Figure 10. ^{1}H NOE spectra of both samples. NOE percent between proton 4a and 8a: **16** <1, **15** 4.0.

carbon NMR spectra for the two isomers is shown in Figure 9a,b. In this figure we assign the positions in the rings for each carbon line. The ^{13}C solid-state NMR spectra for the iodide salts are shown in Figure 9c,d, and these are Cross Polarization Magic Angle Spinning (CP MAS) spectra. While we have not labeled the carbons again, it is straightforward to see the relationship from the solution spectra albeit with some shift in chemical shift and peak broadening occurring for some lines.

We implemented a strategy for assignment of the two isomers built upon a sequence of NMR experiments, which would allow us to make conformation assignments with certainty. The steps were the following:

(a) The use of DEPT (Distortionless Enhancement by Polarization Transfer) experiments allows us to assign the CH, CH$_2$, and CH$_3$ carbons in the molecules. We then assign the important carbon atoms 4a and 8a in relation to later determining cis and trans configurations for the hydrogens bonded to these two bridging carbons.
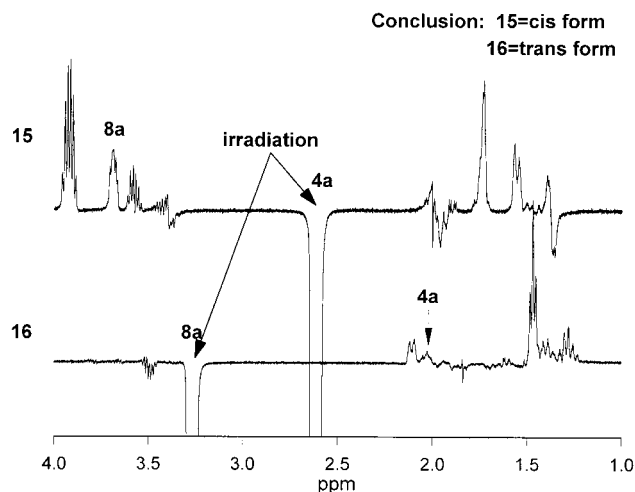
(b) HMQC experiments (Heteronuclear Multiple Quantum Coherence spectroscopy; a 2D sequence for heteronuclear correlation) tell us the ^{1}H$-^{13}$C correlations so that we can map out the H peaks, which are affiliated with the various carbon centers.

(c) ^{1}H COSY experiments (Correlation Spectroscopy; another 2D sequence for homonuclear correlation) let us map out the ^{1}H$-^1$H spin couplings that are two bonds apart. That helps in the assignment of the ^{13}C$-^{13}$C connectivities in the ring structure.

(d) NOE (Nuclear Overhauser Effect) experiments allow us to irradiate selected protons and then see which spatially close atoms are affected.

To get started we collected ^{1}H spectra for each of the iodide salts dissolved in CDCl$_3$ for the two isomers. These data are given in Figure S1, Supporting Information. Some other key proton assignments were then made from the use of HMQC experiments (see Supporting Information, Figure S2a,b). These assignments could then be a basis for complete assignment with use of ^{1}H COSY experiments later. These experiments ought to give us important conformation about key protons such as those for positions 4, 4a, 5, 8, and 8a in the two isomers. The relationship of these protons is the key area where we expect to see differences in the two isomers. The ^{1}H COSY experiments for full range and then just CH$_2$ protons are given for both isomers in the Supporting Information, Figures S3−S6. Figure S7a,b in the Supporting Information gives the DEPT spectra for carbon, allowing us to assign the methine groups in particular. These become important in assigning the protons we want to explore the H−H distance information in the NOE experiment.

Next our task was to determine the cis or trans configuration of protons 4a relative to 8a in the two isomers. This was probed by using the NOE experiment. These data for the two isomers are shown in Figure 10. With particular care we can selectively irradiate one of the protons in the given spectra to measure the resulting enhancement. The irradiation is made on the 4a proton for **15** and the 8a proton for **16** because in each instance these are well separated from other peaks in the ^{1}H NMR spectra. Under the conditions chosen we can see that the response is greatly pronounced for 8a in **15** while the NOE effect is greatly reduced (see the 4a proton) for **16**. In these experiments we
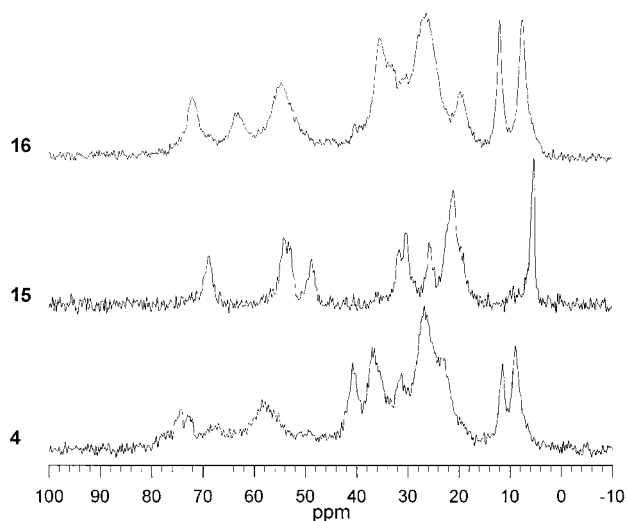
Figure 11. ^{13}C CP MAS spectra of as made zeolite materials using **4**, **15**, and **16**, collected on a Bruker DSX-200 with a contract time of 500 μs and a spinning rate of 4 kHz.

Figure 12. Transmission electron micrograph of SSZ-48 having crystallized from **15** and as a borosilicate sieve.

Figure 13. High-resolution electron micrograph of SSZ-48 rods. The parallel pores (lattice fringes) can be seen in the image.

might expect a typical enhancement of up to about 10%. We obtain a value of about 4% for **15** and less than 1% for **16**. This leads us to conclude a cis configuration for **15** and a trans configuration for **16**, subsequently allowing us to conclude that the cis conformation is the isomer that does indeed lead to the new zeolite SSZ-48. The two isomers are shown in better conformational display in Figure 3 than in Figure 9a,b. Looking at the projections and then at Table 1 we can rationalize why one conformation fits into the 12-ring zeolite, and then why the trans isomer fits well into the large cavity of the 8-ring SSZ-36.

Both CPMAS and Block Decay MAS ^{13}C spectra (Figure 11) were acquired on the as-synthesized zeolites for the use of the two isomers. Spectra were also obtained under the same conditions for **4**. This organocation can be thought of as a homologue of decahydroquinoline with an additional ring CH$_2$ group. **4** has a very high selectivity for SSZ-36. Using a Bruker DSX-200 instrument, the CP MAS spectra were taken with a contact time of 500 μs with a spinning rate of 4 kHz.

A few key conclusions can be reached. First, if we examine the ^{13}C spectra for the solid-state iodide salts and then these spectra, there are changes in the chemical shifts and relative line intensities as well.[26] We must keep in mind that we are looking at single molecules, isolated within the zeolite, and not energy minimized in a packed crystalline organic solid. These changes should be associated with the changes in geometry of the molecule as well as the interaction of the cation with the SiO$_2$ cages while the conformation (cis and trans) should remain the same in the occluded situation. Certainly the external surfaces (as is the case for the methyl groups) have important contacts with the zeolite surfaces as indicated by the clear differences in the chemical shifts and resolution compared to the pure iodide salts. The deviation in chemical shifts seen for both isomers is in general more enhanced for the upfield carbons (usually associated with greater electron density). This information may eventually tell us something about how these single molecules are actually packing in the zeolite cavities (once a zeolite structure is known, it is possible to perform energy-
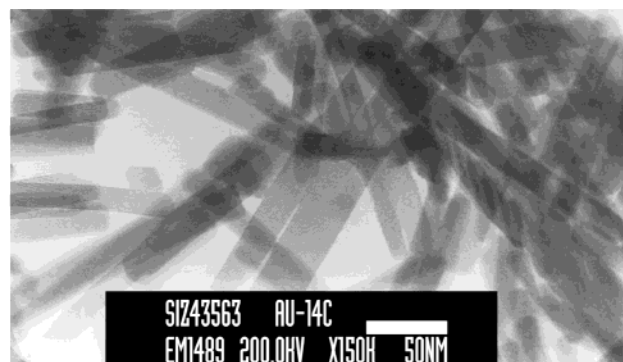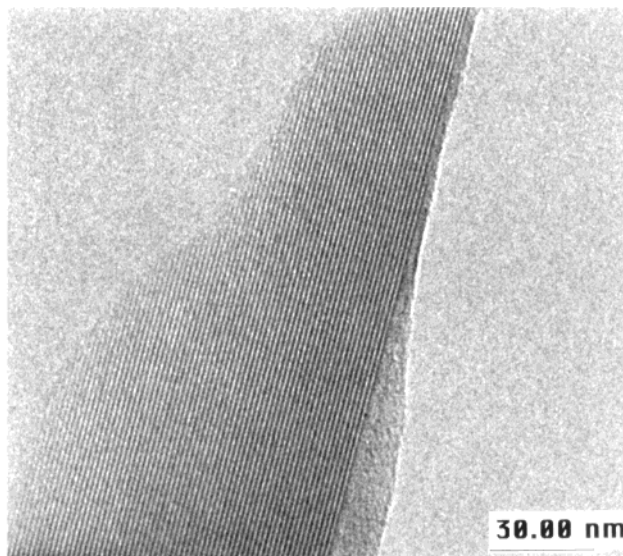
(26) Zones, S. I.; Hwang, S.-J.; Davis, M. E. *Chem. − A Eur. J.* **2001**, *7*, 1999.

minimization calculations for the guest organocations, with certain simplification assumptions being made). Second, in comparing the three spectra, if one starts with **4**, and then using a peak-by-peak comparison, it can be seen that the chemical shifts for **16** track **4** much more closely than **15**. This would be a good indication that **4** also has a trans conformation. In addition, as we pointed out, it has an even better selectivity for SSZ-36 than **16**.

3. SSZ-48 Characterization: A New Product from Beckmann Rearrangement Chemistry. The SSZ-48 crystallizes in fibrous rods from a reaction mixture, which includes sodium borate as the trivalent (lattice-substituting) inorganic source. Figure 12 shows a transmission electron micrograph. An even greater magnification (Figure 13) shows the parallel pore system running down the length of the rods. The initial crystallization took a number of weeks, but subsequent runs could be seeded with this initial product and the crystallization time was reduced to a matter of days. While the product is formed as a borosilicate, removal of the guest molecule by thermal decomposition, followed by solution treatment of the borosilicate with aluminum nitrate, resulted in the aluminosilicate version of this zeolite.[27] The latter possesses much stronger Bronsted acidity and this can be an important parameter for successful use of zeolites as catalysts. Figure 14 is the X-ray powder diffraction pattern, taken using synchrotron radiation. The zeolite was initially described

FB01 SSZ-48 43594 6,8,700

15-NOV-96
03:06:10
DKA100:[BNL.X7ANOV96F]FB01A.DAT;2
DKA100:[BNL.X7ANOV96F]FB01B.DAT;2
DKA100:[BNL.X7ANOV96F]FB01C.DAT;2
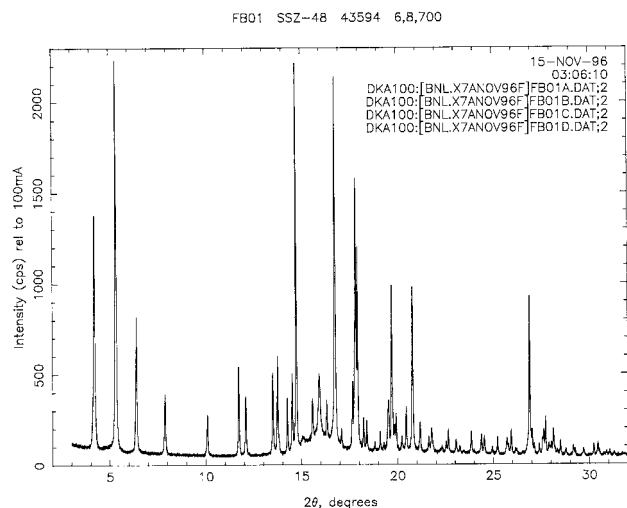DKA100:[BNL.X7ANOV96F]FB01D.DAT;2

Figure 14. X-ray diffraction pattern of zeolite SSZ-48. The data were collected at beamline X7A at the Brookhaven National Laboratory.

as unique from the standpoint that this pattern could not be matched to any other zeolite pattern.

The eventual determination of the zeolite structure came from data taken with a high-resolution electron microscope and the attendant electron diffraction data.[17] This proved to be one of the first times this technique was successfully applied to zeolite structure determination. In the refinement of the new structure, the data must of course be consistent with the X-ray powder diffraction data as well.

Figure 15a shows a topology of the zeolite material, with the cis organocation residing within the pores. The substructure of the zeolite, derived from symmetric connection of silicate rings (alternating Si and O bonds), can be seen. The bulk of the solid can be considered to be derived from sheets made up of organized 5- and 6-ring silicates. Cross-linking these sheets, periodically, with 4-rings generates the zeolite's 12-ring pores, the largest rings observed in the structure. Without the 4-ring "spacers" the zeolite would have a 10-ring pore system.

In an analogous manner, Professor Ken Balkus (Figure 16a) has shown that a 10-ring, 1D zeolite framework (ZSM-48) can be expanded through a σ transformation via insertion of a pair of 4-rings to a 12-ring zeolite (SSZ-31). An additional transformation with another set of 4-rings to aid in the expansion produces the first known 14-ring silicate zeolite, UTD-1.[28] The fascinating concept concerning these transformations is that Professor Balkus' research group actually synthesized all three structures via use of organometallic cations (cobaltacenes) of increasing size. In each instance, the size of the organocation fit the one-dimensional pores rather snugly.

Figure 16b gives a representation of how the SSZ-48 zeolite could be transformed to a 14-ring zeolite by using a single σ transformation. By analogy with the Balkus work, we also show that removal of the 4-rings from SSZ-48 would yield a known 10-ring, of TON topology.[20] A number of organocations have been used in stabilization calculations toward an understanding
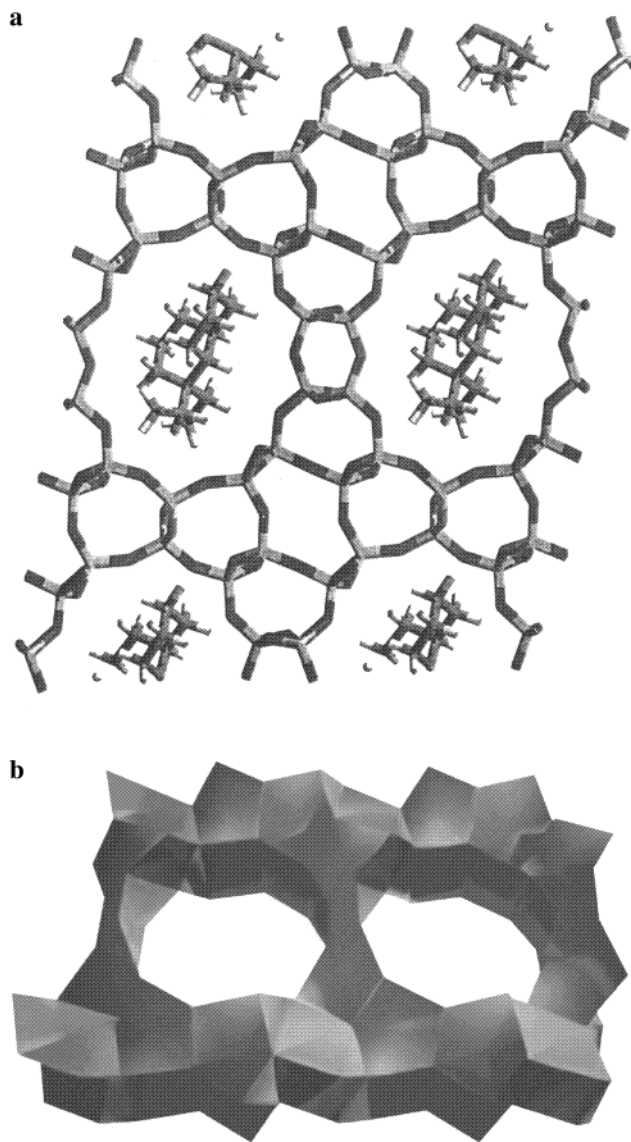
(27) Chen, C. Y.; Zones, S. I. *Proceedings of the 13th International Zeolite Conference*; Montpelier, France, 2001; Vol. 135, Studies in Surface Science and Catalysis; Galarneau, A., Di Renzo, F., Fajula, F., Vedrine, J., Eds.; Elsevier: Amsterdam, The Netherlands.

(28) Balkus, K. J.; Rameraran, A. R.; Szostak, R.; Mitchell, M. *Proceedings of the 12th International Zeolite Conference*; Treacy, M. M. J., Marcus, B. K., Bisher, M. E., Higgins, J. B., Eds.; Material Research Society: Warrendale, PA, 1998; pp 1931−9.

a

b

Figure 15. (a) A representation of organocation, **15**, inside the pores of SSZ-48. (b) A three-dimensional representation of SSZ-48 created in Animation Master and Photoshop from crystalline data supplied by Diamond software.

of structures that might be too large for a guest role in SSZ-48 crystallization, but might lead to the formation of the related 14-ring.[29] Synthesis studies are underway to attempt to make such guest molecules and to verify their structure-directing capabilities in zeolite synthesis.

Conclusions

A series of organocations built around the concept of fused bicyclo compounds were studied in zeolite synthesis. The position of the nitrogen atom in one of the rings influenced the symmetry of the eventual organocation. This was particularly the case in terms of whether an axis could be found passing through the nitrogen atom. Molecules with such a symmetry axis generally produced β zeolite at high lattice substitution and MTW at low levels of substitution. Less symmetric isomers tended to generate "cage-based" zeolite products (e.g. SSZ-35, 36). These same compounds at higher SiO_2/Al_2O_3 synthesis

(29) Wagner, P. Ph.D. Dissertation, California Institute of Technology, Pasadena, CA; 1998.

a

2 s-expansions

ZSM-48   UTD-1
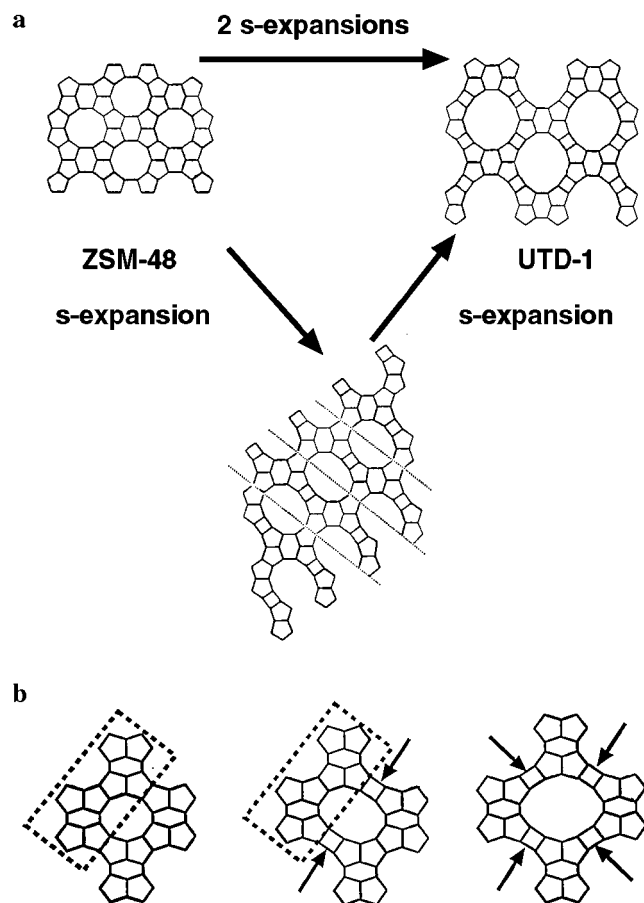
s-expansion   **s-expansion**

b

Figure 16. A schematic of how increasingly larger pore zeolites can be built up by 4-ring insertions into existing structures (σ expansion). Part a shows the known sequence of compounds, 10-ring ZSM-48, onto 12-ring SSZ-31, on 14-ring UTD-1, via successive transformations. Prof. Ken Balkus, Jr., and colleagues succeeded in synthesizing all three zeolites by using increasingly larger cobaltecium SDA. (b) The same σ expansion carried out on 10-ring TON produces SSZ-48. A second change produces a hypothetical 14 ring.

conditions often yielded SSZ-31. This was particularly true for compounds with nitrogen at the 1 or 2 position in the ring. The SSZ-31, while still a 12-ring like MTW, has considerably more distortion in the pore, being an elliptical 12-ring with a long dimension of 8.8 Å. This can better accommodate the "wider", less symmetric templates. The ability to generate different *N*-position isomers was partially a spin-off of using the Beckmann rearrangement reaction on bicycloketones. The generation of SSZ-31 by some candidates also implies that there is a favoring of the incorporation of trans isomers in those experiments; these isomers will more closely approximate the "planar" conformation needed to reside in the 8.8 Å by 5.5 Å pore.

A pair of isomers from *N,N*-diethyldecahydroquinolinium cations were used in zeolite syntheses and a new zeolite, SSZ-48, emerged. The separation of the isomers and their subsequent NMR analysis and then inspection of the SSZ-48 product (by ^{13}C MAS NMR) showed that only the cis isomer was used in the crystallization. Use of the pure trans isomer, **16**, showed a high preference of cage-based zeolite product, SSZ-36. A structurally similar organocation, **4**, showed similar zeolite crystallization selectivity.

The SSZ-48 zeolite structure, largely solved by a breakthrough in electron microscopy approaches,[17] has a 12-ring pore that undulates through the crystal without channel intersection.

15, which accounted for the discovery of this zeolite, also produced two other 12-ring zeolite structures when used in different lattice-substitution contexts.

Balkus and co-workers, for the series ZSM-48/SSZ-31/UTD-1, had observed an earlier set of ring size transitions: (10-ring) to SSZ-31 (12-ring) to UTD-1 (14-ring) using a single σ operation in each step. Each ring size was found by using an increasingly larger cobaltecium cation.[28] In a similar way, SSZ-48 can be seen as the 12-ring that sits between TON as the 10-ring and a hypothetical 14-ring. Each zeolite is separated by a single σ transformation that inserts a pair of 4-rings into the structure, enlarging the main pore by two tetrahedral atoms. Modeling studies have suggested some candidate organocations that could have good selectivity for generating the 14-ring zeolite under the same reaction conditions that have yielded SSZ-48. Studies are underway to synthesize and explore the use of such candidate molecules in zeolite synthesis.

Finally a theme has been continued here from some of our earlier work. Finding a new organic synthesis strategy can serve as an entry into a group of structurally similar organocations. Their exploratory use in zeolite synthesis then serves two functions: First, the researcher has a chance to generate entirely new zeolite structures, and that was seen here for zeolite SSZ-48. This generates the potential for new shape-selective catalysts of value in a variety of molecular processing applications. Second, the various zeolite products, generated by the different homologues made and tried in the study, give a better picture of how guest molecules fill space in crystalline host lattices. This can be particularly helpful for the synthetic chemist when making a zeolite product whose structure is unknown, but is produced by more than one guest molecule.

Supporting Information Available: Figure S1, ^{1}H NMR of two isomer crops of Iodide salts (15, 16) obtained using a Varian INOVA-500 spectrometer with the assignments based on ^{1}H–^{13}C heteronuclear correlation spectroscopy (HMQC sequence) that is shown in Figure S6a,b; Figure S2a, HMQC spectrum of **15**; Figure S2b, HMQC spectrum of **16**; Figure S3, ^{1}H COSY spectrum of **16**: whole range; Figure S4, ^{1}H COSY spectrum of **16**: CH$_2$ groups; Figure S5, ^{1}H COSY spectrum of **15**: whole range; Figure S6, ^{1}H COSY spectrum of **15**: CH$_2$ groups; Figure S7a, ^{13}C 1D and DEPT spectra of **15**, DEPT-90 filters out CH carbons (the DEPT-135 results in positive CH and CH$_3$ and negative CH$_2$ carbons); Figure S7b, ^{13}C DEPT NMR of **16** (PDF). This material is available free of charge via the Internet at http://pubs.acs.org.

JA011513O